ACS APPLIED MATERIALS & INTERFACES

Research Article

Cite This: ACS Appl. Mater. Interfaces 2019, 11, 27134−27144

www.acsami.org

Universal Bipolar Host Materials for Blue, Green, and Red Phosphorescent OLEDs with Excellent Efficiencies and Small-Efficiency Roll-Off

Shimin Hu,[†,∥] Jiajie Zeng,[†,∥] Xiangyu Zhu,[†] Jingjing Guo,[†] Shuming Chen,[‡] Zujin Zhao,*[,†] and Ben Zhong Tang[†,§]

[†]State Key Laboratory of Luminescent Materials and Devices, Center for Aggregation-Induced Emission, South China University of Technology, Guangzhou 510640, China

[‡]Department of Electrical and Electronic Engineering, South University of Science and Technology of China, Shenzhen, Guangdong 518055, China

[§]Department of Chemistry, Hong Kong Branch of Chinese National Engineering Research Center for Tissue Restoration and Reconstruction, The Hong Kong University of Science and Technology, Clear Water Bay, Kowloon, Hong Kong, China

Supporting Information

ABSTRACT: Host materials are indispensable for the fabrication of organic light-emitting diodes (OLEDs) with phosphorescent emitters, but high-quality host materials that can efficiently and simultaneously function in blue, green, and red phosphorescent OLEDs (PHOLEDs) are much rare. In this work, four bipolar materials are developed using carbazole and 9,9-dimethyl-9,10-dihydroacridine as hole-transporting groups, pyridine as electron-transporting groups, and biphenyl and *m*-methylbiphenyl as π-spacers. The crystal and electronic structures indicate that these materials have highly twisted conformations, which endow them with aggregation-induced emission features, intramolecular charge transfer processes, wide energy band gaps, and high triplet energies. The carrier transport ability and energy transfer property analyses show that these materials are able to achieve balanced hole and electron transports and can serve as bipolar host materials for PHOLEDs. A series of monochromatic PHOLEDs with different phosphorescent dopants, including blue-emissive FIrpic, green-emissive $Ir(ppy)_2(acac)$, and red-emissive $Ir(piq)_2(acac)$, are fabricated by employing these four host materials. The green PHOLEDs can provide an impressive luminance of up to 230 200 cd m^{-2}. Based on an identical host material, excellent external quantum efficiencies as high as 25.12, 24.73, and 19.71%, as well as minor efficiency roll-off, are attained for blue, green, and red PHOLEDs, respectively, clearly demonstrating the promising applications as universal bipolar host materials in PHOLEDs with monochromatic light and white light.

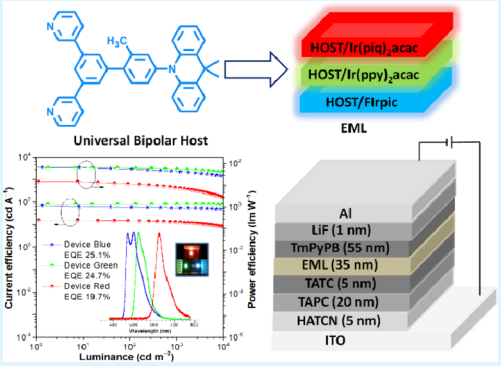

KEYWORDS: *bipolar host, aggregation-induced emission, carrier transport, energy transfer, phosphorescent OLEDs*

1. INTRODUCTION

Owing to the extensive applications in full-color panel displays, organic light-emitting diodes (OLEDs) based on phosphorescent emitters (PHOLEDs) have become one of the most successful advancements in the research field of organic optoelectronic devices.[1,2] Different from fluorescent OLEDs, the internal quantum efficiency of PHOLEDs is much higher, which can theoretically reach 100% in the process of electroluminescence (EL).[3−7] To realize efficient PHOLEDs, phosphorescent emitters are usually dispersed in an appropriate host matrix to constitute the emissive layer to alleviate concentration quenching and depress exciton annihilation processes, for instance, triplet-polaron quenching, singlet−triplet annihilation, and triplet−triplet annihilation (TTA).[8,9] In addition, the adopting of host materials is also conducive to facilitating carrier injection and transport and modulating EL color via energy-transfer mechanism. Therefore, the design of high-quality host materials is of great importance for maximizing EL performance, adapting to the rapid development of various phosphorescent emitters, and fulfilling the increasing requirements of device fabrication technology.

Among various host materials, the innovative bipolar host materials are certified as the most effective candidates so far.[10−13] For these bipolar host materials with donor−acceptor systems, it is feasible to integrate good and comparable hole-transporting and electron-transporting capabilities to achieve

Received: April 22, 2019
Accepted: July 4, 2019
Published: July 4, 2019

DOI: 10.1021/acsami.9b06995
ACS Appl. Mater. Interfaces 2019, 11, 27134−27144

Scheme 1. Synthetic Routes of Bipolar Host Materials DPBP-DMAC, DPMBP-DMAC, DPBP-CZ, and DPMBP-CZ

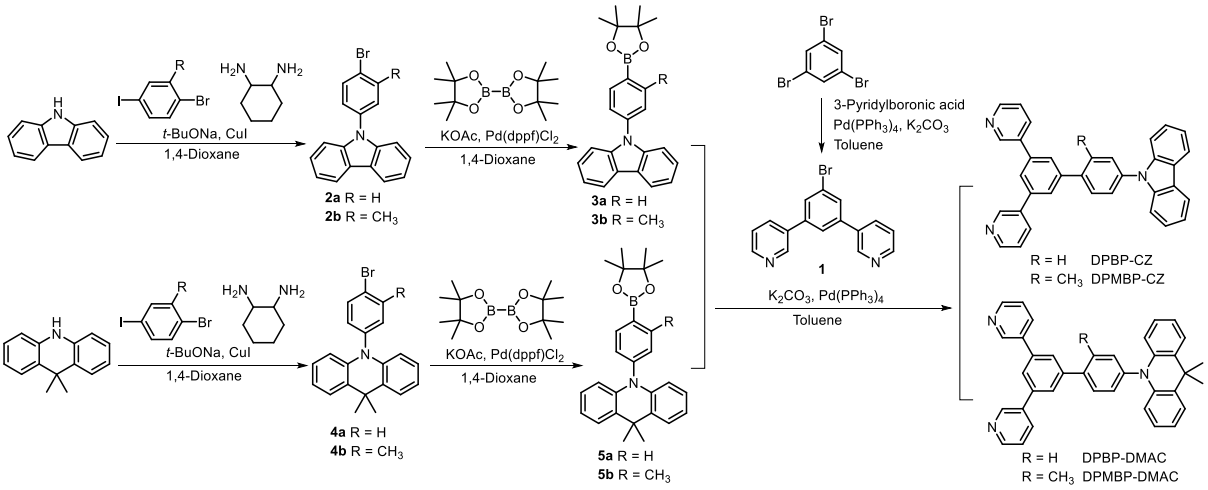

balanced hole and electron fluxes for efficient exciton recombination in OLEDs. Because of the unipolar charge-transporting property of many conventional organic host materials like *m*CP and CBP, the exciton recombination region within the emitting layer (EML) would be narrowed down. The exciton recombination may occur at the interface areas of the EML/hole-transporting layer (HTL) or EML/electron-transporting layer (ETL) of PHOLEDs, resulting in TTA and critical efficiency roll-off at high luminance. Some reports suggest that the efficiency roll-off conundrum can be solved by employing a cohosts system, namely using hole-transporting and electron-transporting hosts at the same time. However, this method complicates the device fabrication processes and increases manufacturing cost and actually is only applicable for certain limited phosphorescent dopants in most cases.[14,15] On the contrary, the carrier injection and transport of bipolar host materials can be more balanced.[16,17] Therefore, the recombination region within EML will become broader, realizing excellent PHOLEDs with high efficiency and faint efficiency roll-off. Therefore, the device configurations and fabrication procedures can be greatly simplified, which is favored to reduce unwanted power loss and cut manufacturing cost.

As the development of scientific research, a great number of bipolar molecules based on electron donor−acceptor systems have been designed as universal host materials to meet the demands of high-performance monochromatic PHOLEDs and even the multilayer white PHOLEDs.[18−22] Under certain circumstances, by adjusting the intramolecular charge-transfer efficiency, the triplet energy as well as energy band gap can be tuned, which can make these bipolar molecules universal hosts for monochromatic PHOLEDs. Generally, an efficient universal host material should simultaneously fulfill following criterias:[23−28] (1) higher triplet levels than those of dopants to astrict the triplet excitons within the phosphorescent emitters; (2) appropriate lowest unoccupied molecular orbital (LUMO) and highest occupied molecular orbital (HOMO) levels of hosts and dopants to assure efficient carrier injection and transport and to increase the exciton recombination; (3) excellent thermal stability to guarantee morphological stability and to prolongate device lifetime. Therefore, the development of high-quality universal host materials is still challenging. Especially, implementing high efficiency and faint efficiency roll-off of monochromatic PHOLEDs with simple and unified architecture is quite difficult. To the best of our knowledge, the first report on the universal bipolar host material was presented by Cheng and Chou,[18] in which the bipolar host material was designed and applied for blue, green, and red PHOLEDs with high EL efficiencies but sharp efficiency roll-off. Recently, several universal bipolar host materials for highly efficient and full-color PHOLEDs with reduced efficiency roll-off have been reported. However, the device configurations were extraordinarily complicated,[15,27] and the specific device structures were needed for different color phosphorescent dopants. Delightfully, Wong et al.[28] explored four bipolar molecules using 1,3,4-oxadiazole as electron-transporting, carbazole (CZ) as hole-transporting, and biphenyl (or *o*-terphenyl) as a bridging linker. They prepared blue, green, yellow, orange, and red PHOLEDs with EL efficiencies of around 20% under a common device structure, using the biolar molecules as universal bipolar host materials. In the study, highly twisted molecular conformations were employed to reduce the electronic coupling effect of the donor−acceptor systems, which had a positive effect on retaining high triplet energy and impeding exciton quenching to realize high device performance.

In this work, four bipolar molecules comprised of electron-transporting pyridine, hole-transporting 9,9-dimethyl-9,10-dihydroacridine (DMAC) and CZ, and different π-spacers of biphenyl (or *m*-methylbiphenyl) are designed and synthesized. We prepared blue, green, and red PHOLEDs, employing these four molecules as universal bipolar host materials. These four molecules are of highly twisted conformations and exhibit aggregation-induced emission (AIE) features,[29−33] high triplet levels, and appropriate HOMO and LUMO energy levels. All the four molecules hold prominent universal bipolar host characteristics and can function as the hosts for blue, green, and red PHOLEDs with a simple and common configuration,[34,35] furnishing excellent EL efficiency and minor efficiency roll-off. Based on an identical host molecule, impressive EL efficiencies of 25.12, 24.73, and 19.71% have been attained for blue, green, and red PHOLEDs, respectively.

2. RESULTS AND DISCUSSION

2.1. Synthesis and Crystal Structures. The specific synthetic routes of new bipolar host materials DPBP-DMAC, DPMBP-DMAC, DPBP-CZ, DPMBP-CZ, and intermediates are illustrated in Scheme 1. All of the compounds were

DOI: 10.1021/acsami.9b06995
ACS Appl. Mater. Interfaces 2019, 11, 27134−27144

synthesized based on Ullmann and Suzuki coupling reactions.[36−40] The target products were obtained via Suzuki coupling reactions between compounds **1** and **3** (or **5**) and characterized by NMR spectroscopy (Figures S1−S8) and high-resolution mass spectrometry. The crystal structures of DPMBP-CZ and DPBP-DMAC, as depicted in Figure 1, show

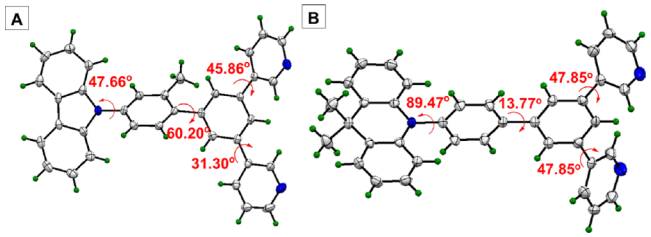

Figure 1. Single-crystal structures with indicated torsion angles of (A) DPMBP-CZ and (B) DPBP-DMAC.

that they adopt a highly twisted conformation. The hole-transporting CZ is attached to the *m*-methylbiphenyl linkage in a twisted manner with a torsion angle of 47.66°. An even larger torsion angle of 89.47° is observed between DMAC and biphenyl linkers, indicating that both moieties are connected almost perpendicularly. Furthermore, the electron-transporting pyridine groups are also deviated from the plane of the biphenyl bridge with torsion angles in the range of 31.30°−47.85° in both molecules. On the other hand, the torsion angle of the biphenyl bridge is increased as the addition of the methyl group, from 13.77° in DPMBP-CZ to 60.20° in DPBP-DMAC, because of the stereorepulsion between the phenyl ring and the methyl group. The noncoplanar conformations can effectively reduce π-conjugation between hole- and electron-transporting groups. Moreover, the highly twisted molecular conformations also prevent close packing of DPMBP-CZ and DPBP-DMAC in crystals, and no strong intermolecular $\pi-\pi$ interactions are found, as illustrated in molecular packing diagrams (Figure S9). The lack of close stacking propensity for these molecules implies that they are prone to form stable morphological films, which is favorable for the device fabrication and operation. In addition, the emission quenching and exciton annihilation can also be alleviated, which is helpful to provide the devices with high efficiencies and faint efficiency roll-off.

2.2. Photophysical Properties. The absorption spectra of DPBP-CZ and DPMBP-CZ are similar with two characteristic absorption bands at around 340 and 300 nm (Figure 2), associated to the absorption of the CZ moiety. Different from DPBP-CZ and DPMBP-CZ, DPBP-DMAC and DPMBP-DMAC show only one obvious absorption band at around 250 nm. The optical band gaps (E_gs) of DPBP-CZ and DPMBP-CZ are 3.51 and 3.53 eV, respectively, calculated from the absorption edges of the UV−vis spectra, which are wider than those of DPBP-DMAC (3.31 eV) and DPMBP-DMAC (3.34 eV) (Table 1). In THF solution (Figure S10), DPBP-CZ exhibits a fluorescence peak at 382 nm, while DPMBP-CZ shows dual fluorescence peaks at 346 and 362 nm, which are apparently blue-shifted because of the more distorted configuration of DPMBP-CZ. Similar blue-shifted fluorescence peak is also found for DPMBP-DMAC (439 nm) relative to DPBP-DMAC (452 nm). On the other hand, DPBP-DMAC and DPMBP-DMAC show red-shifted fluorescence peaks in comparison with DPBP-CZ and DPMBP-CZ, which is

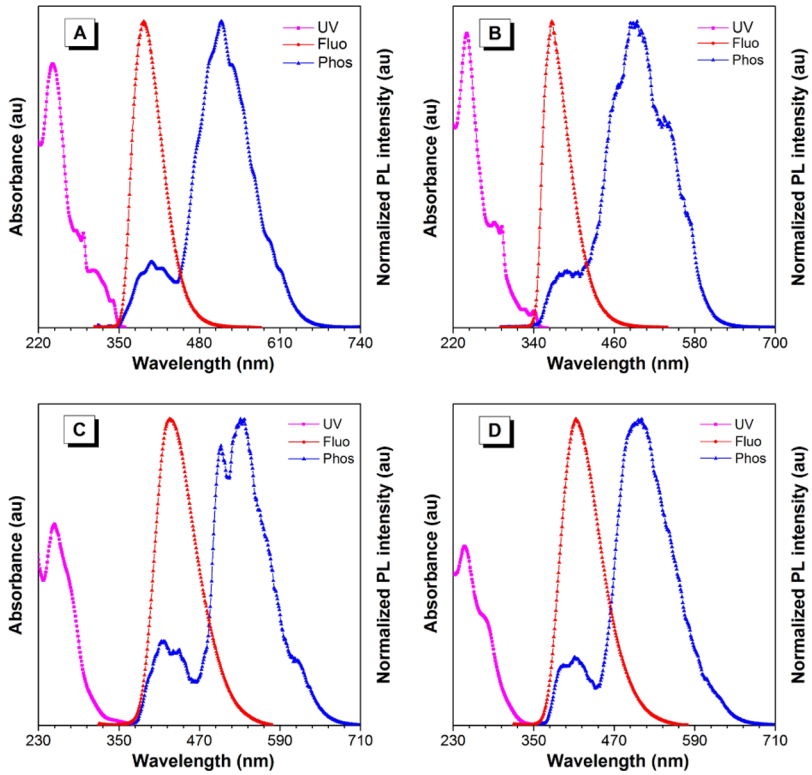

Figure 2. UV−vis absorption, fluorescence, and phosphorescence spectra of (A) DPBP-CZ, (B) DPMBP-CZ, (C) DPBP-DMAC, and (D) DPMBP-DMAC. Absorption spectra were measured in THF solutions (10^{-5} M). Fluorescence spectra were measured in films at room temperature. Phosphorescence spectra were collected in films at 77 K.

DOI: 10.1021/acsami.9b06995
ACS Appl. Mater. Interfaces 2019, 11, 27134−27144

Table 1. Optical Properties, Energy Levels and Thermal Stabilities of the New Bipolar Molecules

compounds	λ_{abs} (nm) soln[a]	λ_{Fl} (nm) soln[a]/film	λ_{Ph} (nm) film[b]	Φ_F (%) soln[a]/film	E_g[c]/E_T[d] (eV)	HOMO/LUMO[e] (eV)	T_g/T_d (°C)
DPBP-CZ	340	382/390	516	6.9/9.9	3.51/2.83	−5.38/−1.87	92/352
DPMBP-CZ	340	346 362/367	491	7.8/14.0	3.53/2.95	−5.40/−1.87	86/344
DPBP-DMAC	254	452/425	534	8.3/12.2	3.31/2.79	−5.29/−1.98	94/347
DPMBP-DMAC	247	439/413	501	8.0/14.5	3.34/2.89	−5.29/−1.95	101/350

[a]In THF solution (10^{-5} M). [b]Measured at 77 K in the film (collected by 5 ms delay). [c]Calculated from onset of the UV−vis absorption spectrum. [d]Calculated from onset of the phosphorescence spectrum of the film. [e]Measured from CV experiments, using Ag/AgCl as the reference in CH_2Cl_2 solution (10^{-3} M).

ascribed to the better electron-donating ability of DMAC than CZ and thus stronger twisted intramolecular charger-transfer (TICT) effect.[41−45] To confirm the TICT effect, the photoluminescence (PL) spectra of DPBP-CZ, DPMBP-CZ, DPBP-DMAC, and DPMBP-DMAC in different solvents with varied polarity were measured (Figure S11). It can be seen that the emission peaks are apparently red-shifted with the increase of solvent polarity, clearly demonstrating their TICT effect.

These molecules in neat films show similar fluorescence behaviors to those in THF solutions, except for slight blue shifts (Table 1, Figure S10. The fluorescence quantum yields of their neat films are higher than their solutions (Table 1), implying that they have AIE properties.[46] The presence of AIE property is instrumental in restraining exciton annihilation in EML and lowering efficiency roll-off of the devices. To better confirm the AIE features of the four molecules, we measured their fluorescence spectra in THF/water mixtures with different water fractions (f_w). The fluorescence spectra of DPMBP-DMAC and the plot of I/I_0 value versus f_w of DPBP-CZ, DPMBP-CZ, DPBP-DMAC, and DPMBP-DMAC are shown in Figure S12. It can be seen that when the f_w is increased from 0 to 70%, the fluorescence of these molecules is decreased and red-shifted, which is owing to the enhanced TICT effect caused by higher solvent polarity. When f_w exceeds 70%, the fluorescence of DPBP-DMAC and DPMBP-DMAC is obviously increased and blue-shifted. Because these materials are insoluble in water, they will form aggregates when the f_w is higher than 70%. The free motion of aromatic groups is restricted by physical constraints in the aggregated state, leading to the block of the nonradiative decay channel and thus fluorescence enhancement.[47−50] On the other hand, both molecules feel weaker polarity in aggregates than in THF solutions, rendering blue-shifted fluorescence.

To evaluate the triplet energy (E_T) values, the phosphorescence spectra of these molecules are collected in films at 77 K. The phosphorescence spectra of these molecules exhibit two similar peaks. A strong long-wavelength peak belongs to the phosphorescence emission, and a weak short-wavelength peak is close to the fluorescence emission, which is probable due to the TTA process. By calculation from the highest energy vibronic sub-band of the phosphorescence spectra, the E_T values of DPBP-CZ and DPMBP-CZ are determined to be 2.83 and 2.95 eV, respectively, and those of DPBP-DMAC and DPMBP-DMAC are 2.79 and 2.89 eV, respectively (Table 1). In comparison with traditional blue phosphorescent dopants, these molecules have higher E_T values, which means that the four molecules can be used as qualified hosts for blue PHOLEDs, let alone green, and red PHOLEDs.

2.3. Theoretical Calculation. In order to gain the energy level information and obtain the optimal molecular structure of these molecules, density functional theory calculation was carried out on DPBP-CZ, DPMBP-CZ, DPBP-DMAC, and DPMBP-DMAC using a B3LYP/6-31G(d,p) basis set. As shown in Figure 3, the optimal molecular structures are similar

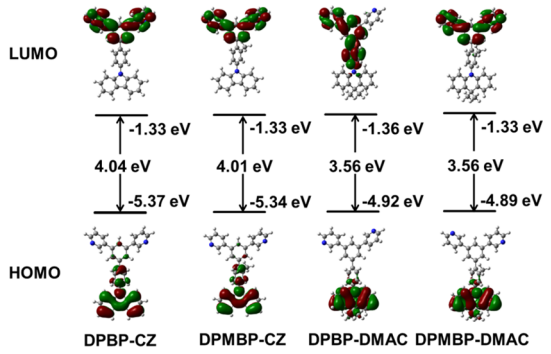

Figure 3. Optimal molecular structures and energy levels of DPBP-CZ, DPMBP-CZ, DPBP-DMAC, and DPMBP-DMAC, calculated by B3LYP/6-31G(d,p).

with the single-crystal structures. It can be observed from the calculated frontier molecular orbitals that all of these molecules have adequate separation HOMOs and LUMOs, due to the highly twisted molecular conformations, which is consistent with the TICT effect of the molecules. The HOMOs are mainly located at CZ and DMAC units, which can provide the hole-transporting channel, while the LUMOs are mainly concentrated on pyridine units, which can contribute to the electron-transporting channel. Moreover, the separation of HOMOs and LUMOs is also particularly crucial for these molecules to ensure their bipolar carrier transport feature as well as high triplet energies.

2.4. Thermal Stability. Good thermal property is very important for the host materials for the fabrication of PHOLEDs. Therefore, the thermal properties of these new molecules are examined by thermogravimetric analysis (TGA) and differential scanning calorimetry (DSC) under a nitrogen atmosphere (scanning rate is 10 °C min^{-1}). As shown in Figure 4, DPMBP-DMAC, DPMBP-CZ, DPBP-DMAC, and DPBP-CZ exhibit good thermal stabilities as evidenced by high decomposition temperatures (T_ds) of 350, 344, 347, and 352 °C at 5% loss of initial weight, respectively. The glass-transition temperatures (T_gs) of DPMBP-DMAC, DPMBP-CZ, DPBP-DMAC, and DPBP-CZ are recorded at 101, 86, 94, and 92 °C, respectively, which are much higher than those of most commonly used hosts *m*CP (60 °C) and CBP (62 °C).[51,52] These results suggest that they have excellent thermal and morphological stabilities, favorable for vacuum evaporation, and conductive to achieving long-lasting PHOLEDs.

2.5. Electrochemical Behaviors. The redox behaviors and the electrochemical stabilities of DPBP-DMAC, DPBP-

DOI: 10.1021/acsami.9b06995
ACS Appl. Mater. Interfaces 2019, 11, 27134−27144

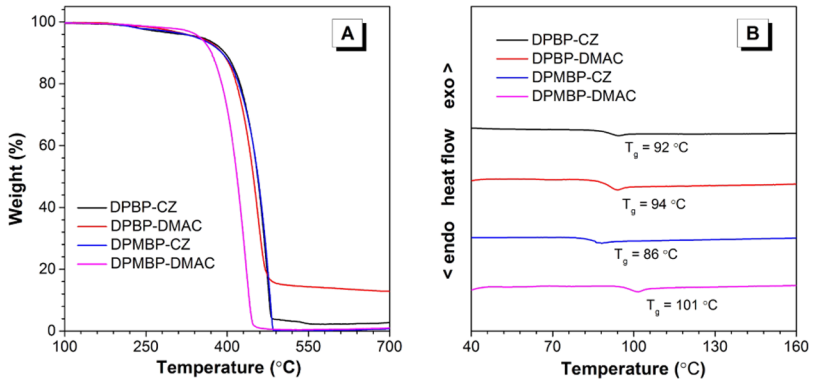

Figure 4. (A) TGA and (B) DSC curves of DPMBP-DMAC, DPMBP-CZ, DPBP-DMAC, and DPBP-CZ, heating rate is 10 °C min^{-1}, and under a nitrogen atmosphere.

CZ, DPMBP-DMAC, and DPMBP-CZ were investigated by cyclic voltammetry (CV) technique. The oxidation and reduction scans were performed in CH_2Cl_2 solution with Bu_4NPF_6 as supporting electrolytes, and the results are shown in Figure 5. For DPBP-CZ, DPMBP-CZ, DPBP-DMAC, and

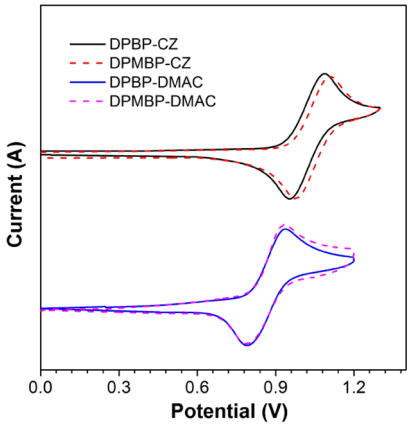

Figure 5. Cyclic voltammograms of DPBP-CZ, DPMBP-CZ, DPBP-DMAC, and DPMBP-DMAC.

DPMBP-DMAC, the onset oxidation potentials (E_{onset}) are at 0.94, 0.96, 0.85, and 0.85 V, respectively. According to the equation of HOMO = $-(E_{onset} + 4.4)$ eV, the HOMO values of DPBP-CZ, DPMBP-CZ, DPBP-DMAC, and DPMBP-DMAC are calculated to be −5.38, −5.40, −5.29, and −5.29 eV, respectively. Calculated from the equation of LUMO = (HOMO + E_g) eV, the LUMO values are −1.87, −1.87, −1.98, and −1.95 eV for DPBP-CZ, DPMBP-CZ, DPBP-DMAC, and DPMBP-DMAC, respectively (E_g is the optical band gap obtained from the absorption onset).

2.6. Electroluminescence. To demonstrate the potential of being universal bipolar host materials in PHOLEDs, DPBP-CZ, DPMBP-CZ, DPBP-DMAC, and DPMBP-DMAC were employed to fabricate several monochromatic devices with different phosphorescent dopants, including blue-emissive FIrpic,[34,51] green-emissive $Ir(ppy)_2(acac)$,[53,54] and red-emissive $Ir(piq)_2(acac)$.[55,56] The devices were fabricated with a configuration of indium tin oxide (ITO)/dipyrazino[2,3-*f*:2′,3′-*h*]quinoxaline-2,3,6,7,10,11-hexacarbonitrile (HATCN) (5 nm)/1,1′-bis(di-4-tolylaminophenyl)cyclohexane (TAPC) (20 nm)/4,4′,4″-tris(carbazol-9-yl)-triphenylamine (TCTA) (5 nm)/host: 10 wt % dopant (35 nm)/1,3,5-tri(mpyrid-3-yl-phenyl)benzene (TmPyPB) (55 nm)/LiF (1 nm)/Al, where DPBP-CZ, DPMBP-CZ, DPBP-DMAC, and DPMBP-DMAC functioned as host materials for devices B1−B4, G1−G4, and R1−R4. The ITO served as the transparent metal-oxide anode, HATCN was used as the hole-injection layer, and LiF was used as the electron-injection layer. TAPC and TCTA were selected as HTL and the electron-blocking layer from EML to HTL. TmPyPB was chosen as ETL and the hole-blocking layer from EML to ETL. The energy level diagrams and the molecular structures of other functional layers used in the devices are depicted in Figure 6, in which the HOMO and LUMO energy values of carrier-transporting materials and dopants are taken

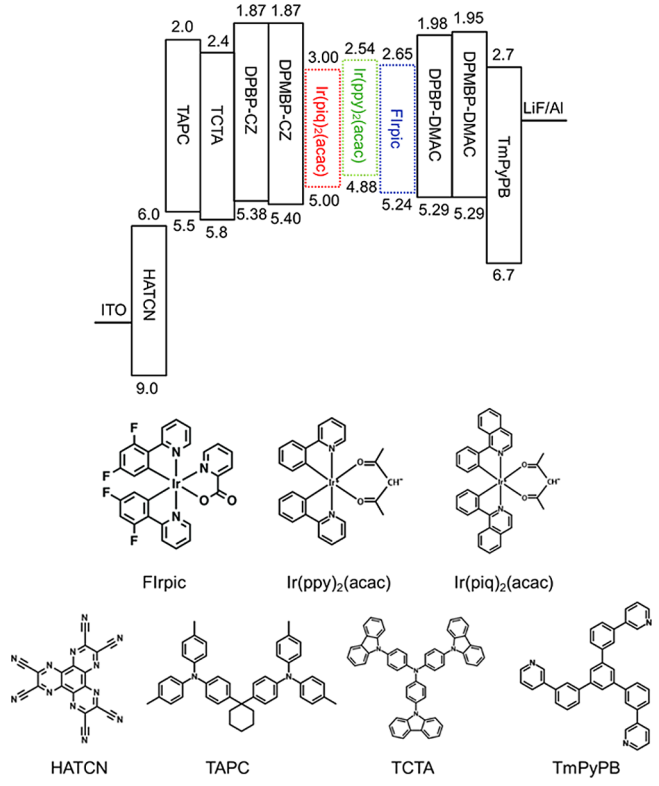

Figure 6. Energy level diagrams (eV) of the devices and molecular structures used in this study. HATCN = dipyrazino[2,3-*f*:2′,3′-*h*]quinoxaline-2,3,6,7,10,11-hexacarbonitrile; TCTA = 4,4′,4″-tris(carbazol-9-yl)-triphenylamine; TAPC = 1,1′-bis(di-4-tolylaminophenyl)cyclohexane; TmPyPB = 1,3,5-tri(mpyrid-3-yl-phenyl)benzene.

DOI: 10.1021/acsami.9b06995
ACS Appl. Mater. Interfaces 2019, 11, 27134−27144

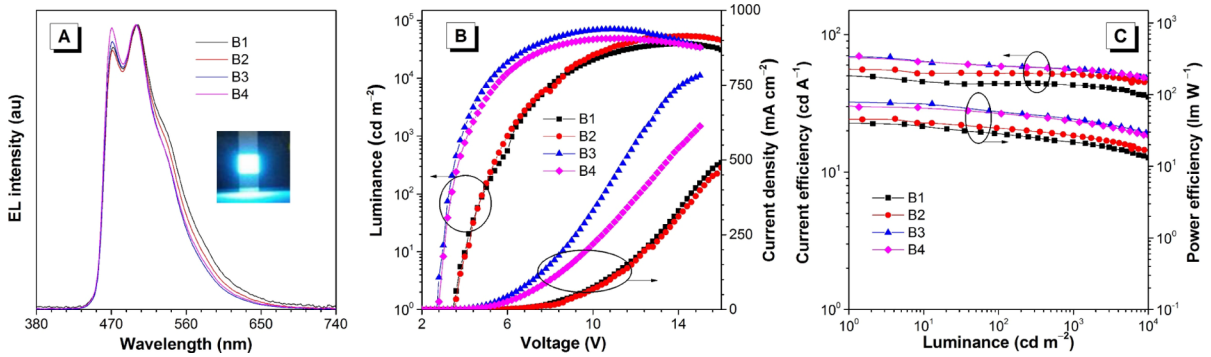

Figure 7. (A) EL spectra of devices B1−B4, measured at 500 cd m^{-2}, (B) luminance and current density changed curves with the change of voltage, and (C) current efficiency and power efficiency changed curves with the change of luminance. DPBP-DMAC (B1), DPBP-CZ (B2), DPMBP-DMAC (B3), and DPMBP-CZ (B4) function as hosts.

Table 2. EL Performances of PHOLEDs Based on the New Bipolar Molecules

device	host	V_{on} [a] (V)	L_{max} (cd m^{-2})	$\eta_{ext,max}$ (%)	$\eta_{C,max}$ (cd A^{-1})	$\eta_{P,max}$ (lm W^{-1})	η_{ext} [b] (%)	CIE [c] (x, y)
B1	DPBP-CZ	3.5	39 660	17.33	44.40	33.20	16.68	(0.215, 0.434)
B2	DPMBP-CZ	3.5	53 930	20.92	52.68	37.59	20.31	(0.204, 0.428)
B3	DPBP-DMAC	2.7	70 800	24.54	59.88	58.76	22.90	(0.194, 0.410)
B4	DPMBP-DMAC	3.3	48 930	25.12	60.67	59.53	22.60	(0.188, 0.407)
G1	DPBP-CZ	3.0	88 540	20.99	73.46	60.85	17.18	(0.411, 0.569)
G2	DPMBP-CZ	2.9	106 000	23.36	89.00	77.62	20.69	(0.361, 0.611)
G3	DPBP-DMAC	3.1	230 200	23.80	85.47	60.99	23.78	(0.306, 0.632)
G4	DPMBP-DMAC	3.1	184 900	24.73	91.51	62.47	24.69	(0.304, 0.639)
R1	DPBP-CZ	3.7	22 800	18.52	12.46	9.32	11.14	(0.681, 0.315)
R2	DPMBP-CZ	3.3	22 980	19.43	13.19	10.90	11.51	(0.682, 0.315)
R3	DPBP-DMAC	2.9	37 110	18.16	13.31	13.06	14.76	(0.681, 0.316)
R4	DPMBP-DMAC	3.7	22 530	19.71	19.48	13.90	15.57	(0.667, 0.322)

[a]The applied voltage required for 1 cd m^{-2}. [b]Recorded at 1000 cd m^{-2}. [c]Recorded at 500 cd m^{-2} (blue and green devices) and 100 cd m^{-2} (red devices).

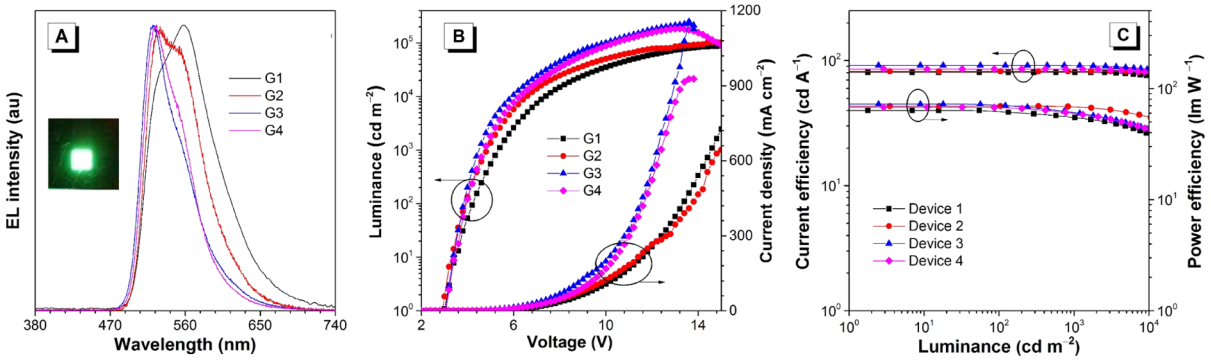

Figure 8. (A) EL spectra of devices G1−G4, measured at 500 cd m^{-2}, (B) luminance and current density changed curves with the change of voltage, and (C) current efficiency and power efficiency changed curves with the change of luminance. DPBP-DMAC (G1), DPBP-CZ (G2), DPMBP-DMAC (G3), and DPMBP-CZ (G4) function as hosts.

from previous literature,[51−57] and the values of these new hosts are determined according to CV measurements (Figure 5).

Compared with green and red PHOLEDs, high-performance blue PHOLEDs are more difficult to achieve because triplet levels of blue phosphorescent materials are generally higher than those of green and red phosphorescent materials. Therefore, we first evaluate the potentials of these bipolar molecules as the host materials in blue PHOLEDs (B1−B4). The EL spectra of devices B1−B4 show pure emissions from FIrpic with fine structures at 470 and 500 nm[58,59] (Figure 7A), without emissions from the host or hole-/ETLs. It suggests that there is no exciton leakage of these devices in the process of energy transfer from hosts to guests. The turn-on voltages (V_{on}, at 1 cd m^{-2}) of B1−B4 are low to 2.7−3.5 V. The low V_{on} can be ascribed to the good match of energy levels among the hosts, dopants, and other organic functional materials. The maximum luminance (L_{max}) values of B1−B4 are as high as 39 660−70 800 cd m^{-2}. Among these four blue PHOLEDs, B4 using DPMBP-DMAC as the host material has the best device performance (Figure 7B,C). The maximum current efficiency ($\eta_{C,max}$), power efficiency ($\eta_{P,max}$), and external quantum efficiency ($\eta_{ext,max}$) of B4 are 60.67 cd A^{-1}, 59.53 lm W^{-1}, and 25.12%, respectively, higher than those of B1, B2, and B3 hosted by DPBP-CZ (44.40 cd A^{-1}, 33.20 lm W^{-1} and

DOI: 10.1021/acsami.9b06995
ACS Appl. Mater. Interfaces 2019, 11, 27134−27144

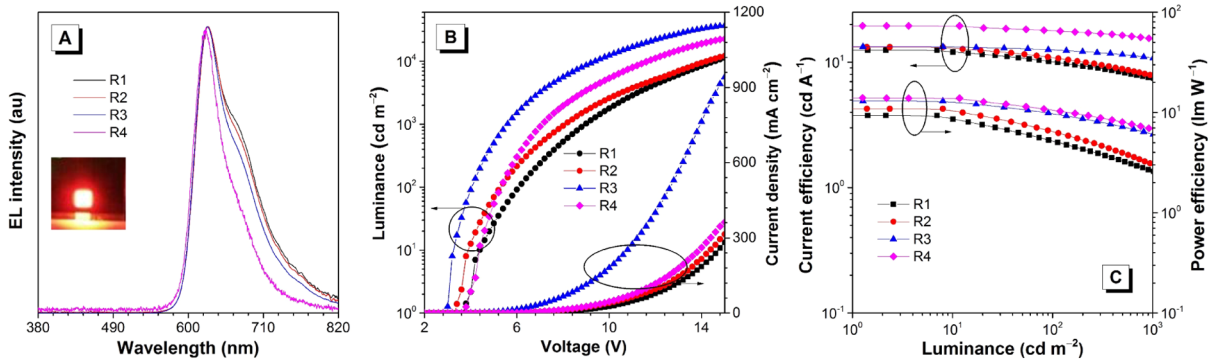

Figure 9. (A) EL spectra of devices R1−R4, measured at 500 cd m^{-2}, (B) luminance and current density changed curves with the change of voltage, and (C) current efficiency and power efficiency changed curves with the change of luminance. DPBP-DMAC (R1), DPBP-CZ (R2), DPMBP-DMAC (R3), and DPMBP-CZ (R4) function as hosts.

17.33%), DPMBP-CZ (52.68 cd A^{-1}, 37.59 lm W^{-1} and 20.92%), and DPBP-DMAC (59.88 cd A^{-1}, 58.76 lm W^{-1} and 24.54%) (Figure S13, Table2). It is worth noting that there are only very limited reports on FIrpic-based PHOLEDs that achieved $\eta_{ext,max}$ over 25%, and the high EL efficiencies of B4 are one of the impressive results of FIrpic-based PHOLEDs ever reported,[60−63] particularly based on the universal hosts. More importantly, the η_{ext} values of B1−B4 are maintained at 16.68, 20.31, 22.90, and 22.60%, respectively, at the high luminance of 1000 cd m^{-2}. The excellent performances of B1−B4 should give the credit to the high triplet energies and balanced carrier transport resulting from the matched electron mobility of pyridine and hole mobility of CZ and DMAC moieties. It is noticeable that the devices B3 and B4 have higher EL efficiencies than B1 and B2. This can be interpreted as that the hosts with the DMAC moiety and *m*-methylbiphenyl linker have more contorted molecular conformations, which are beneficial to provide more balanced carrier transport. In addition, the highly twisted conformations can more efficiently prevent exciton annihilation and emission quenching, which is conductive to improving EL efficiencies and reducing efficiency roll-off.

Next, we evaluate the practical use of these bipolar molecules as the host materials for green phosphorescent Ir(ppy)$_2$(acac) to fabricate PHOLEDs. The generated four green devices G1−G4 also have low V_{on}s at around 3.0 V, thanks to the good match of energy levels. The device G3 that is hosted by DPBP-DMAC reaches an impressive L_{max} of 230 200 cd m^{-2} at 13.6 V (Figure 8). The device G4 using DPMBP-DMAC as the host exhibits the most excellent performance with a $\eta_{C,max}$ of 91.51 cd A^{-1}, a $\eta_{P,max}$ of 62.47 lm W^{-1}, and a $\eta_{ext,max}$ of 24.73%, respectively. At a high luminance of 1000 and 5000 cd m^{-2}, the η_{ext} values are still as high as 24.69 and 23.86%, respectively, demonstrating negligible efficiency roll-off. The devices G1−G3 also reveal good performance with $\eta_{C,max}$s of 73.46, 89.00, and 85.47 cd A^{-1}, $\eta_{P,max}$s of 60.85, 77.62, and 60.99 lm W^{-1}, and $\eta_{ext,max}$s of 20.99, 23.36, and 23.80%, respectively (Table 2).

Lastly, we examine the performance of the four bipolar molecules as the host materials for red phosphorescent Ir(piq)$_2$(acac) to fabricate PHOLEDs. The devices R1−R4 can be turned on at 2.9−3.7 V and radiate red EL peaking at 627 nm from Ir(piq)$_2$(acac) with L_{max} of 22 530−37 110 cd m^{-2}. The device R4 using DPMBP-DMAC as the host gives the best performance with a $\eta_{C,max}$ of 19.48 cd A^{-1}, a $\eta_{P,max}$ of 13.90 lm W^{-1}, and a $\eta_{ext,max}$ of 19.71%, respectively. More importantly, all these red PHOLEDs (Figure 9) demonstrate the remarkable efficiency stability.

In consideration of the excellent EL performances for these monochromatic PHOLEDs, we give credit to sufficiently high E_T[64] and balanced carrier transport[65,66] of the host materials. For the four host materials, the highly twisted geometric conformations can reduce the degree of π-conjugation to retain a high triplet energy and impede exciton quenching[67] by reducing intermolecular $\pi-\pi$ interactions. Among all the monochromatic devices, it is found that the devices hosted by the mostly twisted DPMBP-DMAC furnish the best $\eta_{ext,max}$ values (25.12% for blue PHOLED, 24.73% for green PHOLED, and 19.71% for red PHOLED). The successful demonstration of the excellent efficiencies and wide-range color of PHOLEDs discloses that high color-rendering white-emitting OLEDs can be anticipated by codepositing these hosts and complementary RGB dopants.

2.7. Charge Carrier Mobility. To confirm the bipolar behavior of the hosts, the carrier transport ability of these host materials is investigated by employing SCLC methods.[68,69] The hole-only devices were fabricated with a configuration of ITO/host (80 nm)/TAPC (10 nm)/Al, and electron-only devices were fabricated with a configuration of ITO/TmPyPB (10 nm)/host (80 nm)/LiF (1 nm)/Al. The current density changed curves with the change of voltage ($J-V$) of these devices are illustrated in Figure S14. When the voltage is low, the $J-V$ curves present ohmic characteristics. The current is quadratically dependent on the applied voltage, and it will become space-charge limited, along with applied voltage raising. As displayed in Figure 10, the electron mobility of these four molecules increases in the order of DPMBP-CZ < DPMBP-DMAC < DPBP-CZ < DPBP-DMAC, and the hole mobility of these four molecules increases in the order of DPMBP-CZ < DPBP-CZ < DPMBP-DMAC < DPBP-DMAC. According to the studies, it can be concluded that DPBP-DMAC and DPMBP-DMAC have more balanced electron and hole mobility, leading to the better bipolar feature.

2.8. Energy Transfer. For all the doped PHOLEDs, efficient energy transfer is a crucial factor that gives rise to excellent EL performance. The EL emissions of the hosts, such as DPBP-DMAC (430 nm) and DPMBP-DMAC (416 nm) (Figure S15, Table S1), are not observed in all the doped PHOLEDs, implying complete energy transfer from hosts to guests. To further understand the energy-transfer mechanism, we use the Förster energy transfer radius (R_0), the Förster energy transfer efficiency (Φ_{ET}), and the Förster energy

DOI: 10.1021/acsami.9b06995
ACS Appl. Mater. Interfaces 2019, 11, 27134−27144

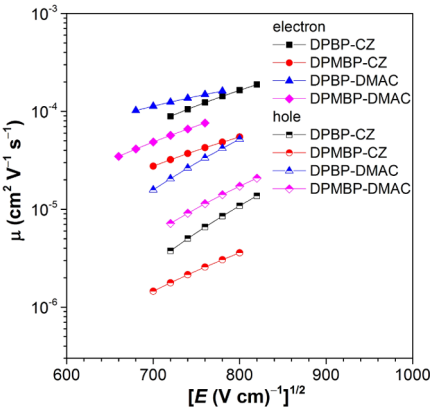

Figure 10. Hole and electron mobility changed curves with the change of $E^{1/2}$ values for DPBP-CZ, DPMBP-CZ, DPBP-DMAC, and DPMBP-DMAC.

transfer rate (k_{ET}) to depict the Förster energy transfer, and we use the distance between the host (D) and guest (A) (R_{DA}) to depict the Dexter energy transfer of the doping PHOLED system. For example, the energy transfer parameters of the dopant FIrpic with different host systems and the host DPMB-DMAC with different dopant systems are listed in Table 3 (details of energy transfer calculations are given in Supporting Information). Obviously, for dopant FIrpic, the Förster energy transfer efficiency and the rate of the FIrpic: DPMBP-DMAC system are higher than those of DPBP-CZ, DPMBP-CZ, and DPBP-DMAC hosts, which is in good agreement with the device performance of devices B1−B4. The device B4 based on the FIrpic: DPMBP-DMAC system shows the highest energy transfer rate and efficiency from the host to the guest, leading to the best device efficiency. Remarkably, for the host DPMBP-DMAC, all of the guest: host systems have high Φ_{ET} and k_{ET} values, indicating efficient energy transfer between DPMBP-DMAC and different guests. These results demonstrate that DPMBP-DMAC is an ideal universal host material.

Different from Förster energy transfer, Dexter energy transfer depends on the shorter distance between the hosts and guests. Now, assuming an ideal host−guest system, the guest molecules are perfectly dispersed in the hosts, namely the dopant molecules should be located adjacent to the host molecules. More concretely, two dopant molecules are expected to locate between two host molecules.[70] Further assuming molecule sizes of both host and guest molecules are 1 nm, and the van der Waals interaction distance is 3 Å,[71] then, the distance between two guests R_{AA} will be about 36 Å ($r_A/2 + r_A/2 + r_D + r_D + 2 \times 3$ Å). It means that 36 Å is the critical value to determine the Dexter energy transfer efficiency. If the distance between two adjacent guest molecules is less than 36 Å, the energy transfer from the hosts to the dopants via the Dexter process can be efficiently achieved. The average distance between guests (R_{AA}) in this work is listed in Table 3. It can be seen that all the R_{AA} values are smaller than 3.6 nm, meaning that the Dexter energy transfer can efficiently occur in these doping systems. These results reveal that both Förster energy transfer and Dexter energy transfer, from the hosts to the guests, contribute to the excellent performance of the devices, especially those with DPMBP-DMAC as the host.

3. CONCLUSIONS

In summary, four universal bipolar host materials with AIE properties are synthesized and systematically characterized. They have twisted geometric conformations as confirmed by X-ray diffraction analysis, which endow them with a stable morphology and sufficiently high E_T values. A series of blue, green, and red PHOLEDs with low driving voltages, high luminance, excellent efficiencies, and very small efficiency roll-off are attained by doping various phosphorescent emitters into these host materials in a simple and common device configuration. All the PHOLEDs show very low turn-on voltages (2.7−3.7 V) and radiate intense light, and the green PHOLEDs can provide an impressive L_{max} of 230 200 cd m^{-2} at 13.6 V. The PHOLEDs based on DPMBP-DMAC and DPMBP-CZ with a *m*-methylbiphenyl linker show better performance than those based on DPBP-DMAC and DPBP-CZ with a biphenyl linker, and the PHOLEDs based on DPMBP-DMAC and DPBP-DMAC have better performances than those based on DPMBP-CZ and DPBP-CZ. This is because the DMAC and the *m*-methylbiphenyl linker are beneficial to improve triplet energy and bipolar transport property due to a highly twisted molecular conformation. Among all the devices, the devices hosted by DPMBP-DMAC possess best balanced carrier mobility and highest energy transfer rate and efficiency and thus provide the best EL efficiencies of 25.12, 24.73, and 19.71% for blue, green, and red PHOLEDs, respectively. DPMBP-DMAC is among state-of-the-art universal bipolar host materials that are practically feasible for full-color PHOLEDs ever reported. The outstanding device performances demonstrate the great potential of these molecules as universal host materials for the potential applications in PHOLEDs with wide-range color. In addition, they may also be promising host materials for blue, green, and red dopants simultaneously for the fabrication of white PHOLEDs.

4. EXPERIMENTAL SECTION

Device fabrication: Multilayer PHOLEDs were fabricated by the vacuum-deposition method. Organic layers were deposited by high-vacuum (5×10^{-4} Pa) thermal evaporation onto a glass substrate precoated with an ITO layer served as the transparent metal-oxide anode. All organic layers were deposited sequentially. HATCN was used as the hole-injection layer, TAPC and TcTa were used as hole-transporting as well as the exciton-block layers, EMLs were comprised of a single host of DPBP-CZ, DPMBP-CZ, DPBP-DMAC, or

Table 3. Energy Transfer Parameters of the Doping Systems

host	Dopant	R_0 (nm)	R_{DA} (nm)	R_{AA} (nm)	k_{ET} ($\times 10^9$ s^{-1})	Φ_{ET} (%)
DPBP-CZ	FIrpic	2.01	1.41	2.30	5.22	89.65
DPMBP-CZ	FIrpic	2.04	1.42	2.32	5.96	90.57
DPBP-DMAC	FIrpic	2.13	1.40	2.30	8.19	92.56
DPMBP-DMAC	FIrpic	2.26	1.40	2.30	11.7	94.62
DPMBP-DMAC	Ir(ppy)$_2$(acac)	2.30	1.34	2.20	17.4	96.36
DPMBP-DMAC	Ir(piq)$_2$(acac)	2.13	1.40	2.33	8.06	92.46

DOI: 10.1021/acsami.9b06995
ACS Appl. Mater. Interfaces 2019, 11, 27134−27144

DPMBP-DMAC with 10 wt % of corresponding dopant [FIrpic, $Ir(ppy)_2(acac)$ or $Ir(piq)_2(acac)$], TmPyPB was chosen as ETL and the hole-blocking layer, and LiF/Al was used as the cathode. The thermal deposition rates for the organic materials, LiF, and Al were 1.0, 0.1, and 10 Å s^{-1}, respectively. The active area of each device was 9 mm^2.

■ ASSOCIATED CONTENT

Supporting Information

The Supporting Information is available free of charge on the ACS Publications website at DOI: 10.1021/acsami.9b06995.

General information, synthesis and characterization, crystal data, energy transfer calculation, NMR spectra, crystal packing illustration, PL spectra, and device character curves and data (PDF)
Crystal data for DPBP-DMAC (CIF)
Crystal data for DPMBP-CZ (CIF)

■ AUTHOR INFORMATION

Corresponding Author

*E-mail: mszjzhao@scut.edu.cn.

ORCID

Shuming Chen: 0000-0001-5218-3257
Zujin Zhao: 0000-0002-0618-6024
Ben Zhong Tang: 0000-0002-0293-964X

Author Contributions

‖S.H. and J.Z. contributed equally to the work.

Notes

The authors declare no competing financial interest.

■ ACKNOWLEDGMENTS

This work was financially supported by the National Natural Science Foundation of China (21788102), the Nation Key Basic Research and Development Program of China (973 program, 2015CB655004) Founded by MOST, the Guangdong Natural Science Funds for Distinguished Young Scholar (2014A030306035), and the Science and Technology Program of Guangzhou (201804020027).

■ REFERENCES

(1) Tang, C. W.; VanSlyke, S. A. Organic Electroluminescent Diodes. *Appl. Phys. Lett.* **1987**, *51*, 913−915.
(2) D'Andrade, B. W.; Forrest, S. R. White Organic Light-Emitting Devices for Solid-State Lighting. *Adv. Mater.* **2004**, *16*, 1585−1595.
(3) Baldo, M. A.; O'brien, D. F.; You, Y.; Shoustikov, A.; Sibley, S.; Thompson, M. E.; Forrest, S. R. Highly Efficient Phosphorescent Emission from Organic Electroluminescent Devices. *Nature* **1998**, *395*, 151−154.
(4) Baldo, M. A.; Lamansky, S.; Burrows, P. E.; Thompson, M. E.; Forrest, S. R. Very High-Efficiency Green Organic Light-Emitting Devices Based on Electrophosphorescence. *Appl. Phys. Lett.* **1999**, *75*, 4−6.
(5) Baldo, M. A.; Adachi, C.; Forrest, S. R. Transient Analysis of Organic Electrophosphorescence. II. Transient Analysis of Triplet-Triplet Annihilation. *Phys. Rev. B: Condens. Matter Mater. Phys.* **2000**, *62*, 10967.
(6) Han, C.; Zhu, L.; Li, J.; Zhao, F.; Zhang, Z.; Xu, H.; Deng, Z.; Ma, D.; Yan, P. Highly Efficient Multifluorenyl Host Materials with Unsymmetrical Molecular Configurations and Localized Triplet States for Green and Red Phosphorescent Devices. *Adv. Mater.* **2014**, *26*, 7070−7077.
(7) Yu, D.; Zhao, F.; Han, C.; Xu, H.; Li, J.; Zhang, Z.; Deng, Z.; Ma, D.; Yan, P. Ternary Ambipolar Phosphine Oxide Hosts Based on Indirect Linkage for Highly Efficient Blue Electrophosphorescence: Towards High Triplet Energy, Low Driving Voltage and Stable Efficiencies. *Adv. Mater.* **2012**, *24*, 509−514.
(8) Ho, C.-L.; Chi, L.-C.; Hung, W.-Y.; Chen, W.-J.; Lin, Y.-C.; Wu, H.; Mondal, E.; Zhou, G.-J.; Wong, K.-T.; Wong, W.-Y. Carbazole-Based Coplanar Molecule (CmInF) as a Universal Host for Multi-Color Electrophosphorescent Devices. *J. Mater. Chem.* **2012**, *22*, 215−224.
(9) Li, J.; Ding, D.; Tao, Y.; Wei, Y.; Chen, R.; Xie, L.; Huang, W.; Xu, H. A Significantly Twisted Spirocyclic Phosphine Oxide as a Universal Host for High-Efficiency Full-Color Thermally Activated Delayed Fluorescence Diodes. *Adv. Mater.* **2016**, *28*, 3122−3130.
(10) Kim, D.; Coropceanu, V.; Brédas, J.-L. Design of Efficient Ambipolar Host Materials for Organic Blue Electrophosphorescence: Theoretical Characterization of Hosts Based on Carbazole Derivatives. *J. Am. Chem. Soc.* **2011**, *133*, 17895−17900.
(11) Chaskar, A.; Chen, H.-F.; Wong, K.-T. Bipolar Host Materials: A Chemical Approach for Highly Efficient Electrophosphorescent Devices. *Adv. Mater.* **2011**, *23*, 3876−3895.
(12) Chen, Y.; Wei, X.; Cao, J.; Huang, J.; Gao, L.; Zhang, J.; Su, J.; Tian, H. Novel Bipolar Indole-Based Solution-Processed Host Material for Efficient Green and Red Phosphorescent OLEDs. *ACS Appl. Mater. Interfaces* **2017**, *9*, 14112−14119.
(13) Lee, C. W.; Lee, J. Y. High Quantum Efficiency in Solution and Vacuum Processed Blue Phosphorescent Organic Light Emitting Diodes Using a Novel Benzofuropyridine-Based Bipolar Host. *Adv. Mater.* **2013**, *25*, 596−600.
(14) Tsai, M.-H.; Lin, H.-W.; Su, H.-C.; Ke, T.-H.; Wu, C.-C.; Fang, F.-C.; Liao, Y.-L.; Wong, K.-T.; Wu, C.-I. Highly Efficient Organic Blue Electrophosphorescent Devices Based on 3,6-Bis(triphenylsilyl)-carbazole as the Host. *Adv. Mater.* **2006**, *18*, 1216−1220.
(15) Sasabe, H.; Toyota, N.; Nakanishi, H.; Ishizaka, T.; Pu, Y.-J.; Kido, J. 3,3'-Bicarbazole-Based Host Materials for High-Efficiency Blue Phosphorescent OLEDs with Extremely Low Driving Voltage. *Adv. Mater.* **2012**, *24*, 3212−3217.
(16) Su, S.-J.; Sasabe, H.; Takeda, T.; Kido, J. Pyridine-Containing Bipolar Host Materials for Highly Efficient Blue Phosphorescent OLEDs. *Chem. Mater.* **2008**, *20*, 1691−1693.
(17) Jeon, S. O.; Yook, K. S.; Joo, C. W.; Lee, J. Y. High-Efficiency Deep-Blue-Phosphorescent Organic Light-Emitting Diodes Using a Phosphine Oxide and a Phosphine Sulfide High-Triplet-Energy Host Material with Bipolar Charge-Transport Properties. *Adv. Mater.* **2010**, *22*, 1872−1876.
(18) Chou, H.-H.; Cheng, C.-H. A Highly Efficient Universal Bipolar Host for Blue, Green, and Red Phosphorescent OLEDs. *Adv. Mater.* **2010**, *22*, 2468−2471.
(19) Gong, S.; Chen, Y.; Luo, J.; Yang, C.; Zhong, C.; Qin, J.; Ma, D. Bipolar Tetraarylsilanes as Universal Hosts for Blue, Green, Orange, and White Electrophosphorescence with High Efficiency and Low Efficiency Roll-Off. *Adv. Funct. Mater.* **2011**, *21*, 1168−1178.
(20) Mondal, E.; Hung, W.-Y.; Dai, H.-C.; Wong, K.-T. Fluorene-Based Asymmetric Bipolar Universal Hosts for White Organic Light Emitting Devices. *Adv. Funct. Mater.* **2013**, *23*, 3096−3105.
(21) Wang, X.; Wang, S.; Ma, Z.; Ding, J.; Wang, L.; Jing, X.; Wang, F. Solution-Processible 2,2′-Dimethyl-biphenyl Cored Carbazole Dendrimers as Universal Hosts for Efficient Blue, Green, and Red Phosphorescent OLEDs. *Adv. Funct. Mater.* **2014**, *24*, 3413−3421.
(22) Ding, L.; Dong, S.-C.; Jiang, Z.-Q.; Chen, H.; Liao, L.-S. Orthogonal Molecular Structure for Better Host Material in Blue Phosphorescence and Larger OLED White Lighting Panel. *Adv. Funct. Mater.* **2015**, *25*, 645−650.
(23) Lin, J.-J.; Liao, W.-S.; Huang, H.-J.; Wu, F.-I.; Cheng, C.-H. A Highly Efficient Host/Dopant Combination for Blue Organic Electrophosphorescence Devices. *Adv. Funct. Mater.* **2008**, *18*, 485−491.
(24) Hwu, T.-Y.; Tsai, T.-C.; Hung, W.-Y.; Chang, S.-Y.; Chi, Y.; Chen, M.-H.; Wu, C.-I.; Wong, K.-T.; Chi, L.-C. An Electron-Transporting Host Material Compatible with Diverse Triplet Emitters Used for Highly Efficient Red- and Green-Electrophosphorescent Devices. *Chem. Commun.* **2008**, 4956−4958.

(25) Sasabe, H.; Kido, J. Development of High Performance OLEDs for General Lighting. *J. Mater. Chem. C* **2013**, *1*, 1699−1707.
(26) Hung, W.-Y.; Chi, L.-C.; Chen, W.-J.; Mondal, E.; Chou, S.-H.; Wong, K.-T.; Chi, Y. A Carbazole−Phenylbenzimidazole Hybrid Bipolar Universal Host for High Efficiency RGB and White PHOLEDs with High Chromatic Stability. *J. Mater. Chem.* **2011**, *21*, 19249−19256.
(27) Xiang, W.; Chang, Y. L.; Lu, J. S.; Zhang, T.; Lu, Z. H.; Wang, S. Bright Blue and White Electrophosphorescent Triarylboryl-functionalized ĈN-chelate Pt(ii) Compounds: Impact of Intramolecular Hydrogen Bonds and Ancillary Ligands. *Adv. Funct. Mater.* **2014**, *24*, 1911−1927.
(28) Cheng, S.-H.; Hung, W.-Y.; Cheng, M.-H.; Chen, H.-F.; Lee, G.-H.; Chung, C.-L.; Yeh, T.-C.; Tang, W.-C.; Huang, S.-L.; Wong, K.-T. Highly Twisted Carbazole-Oxadiazole Hybrids as Universal Bipolar Hosts for High Efficiency PHOLEDs. *Adv. Electron. Mater.* **2016**, *2*, 1500241.
(29) Mei, J.; Leung, N. L. C.; Kwok, R. T. K.; Lam, J. W. Y.; Tang, B. Z. Aggregation-Induced Emission: Together We Shine, United We Soar! *Chem. Rev.* **2015**, *115*, 11718−11940.
(30) Zhao, Z.; Lam, J. W. Y.; Tang, B. Z. T. A Versatile AIE Building Block for the Construction of Efficient Luminescent Materials for Organic Light-Emitting Diodes. *J. Mater. Chem.* **2012**, *22*, 23726−23740.
(31) Chen, B.; Zhang, H.; Luo, W.; Nie, H.; Hu, R.; Qin, A.; Zhao, Z.; Tang, B. Z. Oxidation-Enhanced Emission: Exploring Novel AIEgens from Thieno[3,2-b]thiophene S,S-dioxide. *J. Mater. Chem. C* **2017**, *5*, 960−968.
(32) Zhuang, Z.; Bu, F.; Luo, W.; Peng, H.; Chen, S.; Hu, R.; Qin, A.; Zhao, Z.; Tang, B. Z. Steric, Conjugation and Electronic Impacts on the Photoluminescence and Electroluminescence Properties of Luminogens Based on Phosphindole Oxide. *J. Mater. Chem. C* **2017**, *5*, 1836−1842.
(33) Chen, B.; Nie, H.; Hu, R.; Qin, A.; Zhao, Z.; Tang, B. Z. Insights into the Correlation between the Molecular Conformational Change and AIE Activity of 2,5-Bis(dimesitylboryl)-3,4-diphenylsiloles. *J. Mater. Chem. C* **2016**, *4*, 7541−7545.
(34) Liu, X.-Y.; Tang, X.; Zhao, Y.; Zhao, D.; Fan, J.; Liao, L.-S. Spirobi [dibenzo[b,e][1,4]azasiline]: A Novel Platform for Host Materials in Highly Efficient Organic Light-Emitting Diodes. *J. Mater. Chem. C* **2018**, *6*, 1023−1030.
(35) Chen, W.-C.; Yuan, Y.; Zhu, Z.-L.; Ni, S.-F.; Jiang, Z.-Q.; Liao, L.-S.; Wong, F.-L.; Lee, C.-S. A Novel Spiro-Annulated Benzimidazole Host for Highly Efficient Blue Phosphorescent Organic Light-Emitting Devices. *Chem. Commun.* **2018**, *54*, 4541−4544.
(36) Kim, M. K.; Kwon, J.; Kwon, T.-H.; Hong, J.-I. A Bipolar Host Containing 1,2,3-Triazole for Realizing Highly Efficient Phosphorescent Organic Light-Emitting Diodes. *New J. Chem.* **2010**, *34*, 1317−1322.
(37) Park, I. S.; Lee, S. Y.; Adachi, C.; Yasuda, T. Full-Color Delayed Fluorescence Materials Based on Wedge-Shaped Phthalonitriles and Dicyanopyrazines: Systematic Design, Tunable Photophysical Properties, and OLED Performance. *Adv. Funct. Mater.* **2016**, *26*, 1813−1821.
(38) Liu, M.; Su, S.-J.; Jung, M.-C.; Qi, Y.; Zhao, W.-M.; Kido, J. Hybrid Heterocycle-Containing Electron-Transport Materials Synthesized by Regioselective Suzuki Cross-Coupling Reactions for Highly Efficient Phosphorescent OLEDs with Unprecedented Low Operating Voltage. *Chem. Mater.* **2012**, *24*, 3817−3827.
(39) Monnier, F.; Taillefer, M.; Catalytic, C.-C. Catalytic C-C, C-N, and C-O Ullmann-Type Coupling Reactions. *Angew. Chem., Int. Ed.* **2009**, *48*, 6954−6971.
(40) Li, Y.; Li, X.-L.; Cai, X.; Chen, D.; Liu, X.; Xie, G.; Wang, Z.; Wu, Y.-C.; Lo, C.-C.; Lien, A.; Peng, J.; Cao, Y.; Su, S.-J. Deep Blue Fluorophores Incorporating Sulfone-Locked Triphenylamine: The Key for Highly Efficient Fluorescence−Phosphorescence Hybrid White OLEDs with Simplified Structure. *J. Mater. Chem. C* **2015**, *3*, 6986−6996.
(41) Guo, J.; Li, X.-L.; Nie, H.; Luo, W.; Gan, S.; Hu, S.; Hu, R.; Qin, A.; Zhao, Z.; Su, S.-J.; Tang, B. Z. Achieving High-Performance Nondoped OLEDs with Extremely Small Efficiency Roll-Off by Combining Aggregation-Induced Emission and Thermally Activated Delayed Fluorescence. *Adv. Funct. Mater.* **2017**, *27*, 1606458.
(42) Guo, J.; Li, X.-L.; Nie, H.; Luo, W.; Hu, R.; Qin, A.; Zhao, Z.; Su, S.-J.; Tang, B. Z. Robust Luminescent Materials with Prominent Aggregation-Induced Emission and Thermally Activated Delayed Fluorescence for High-Performance Organic Light-Emitting Diodes. *Chem. Mater.* **2017**, *29*, 3623−3631.
(43) Guo, J.; Hu, S.; Luo, W.; Hu, R.; Qin, A.; Zhao, Z.; Tang, B. Z. A novel Aggregation-Induced Emission Platform from 2,3-Diphenylbenzo[b]thiophene S,S-dioxide. *Chem. Commun.* **2017**, *53*, 1463−1466.
(44) Huang, J.; Nie, H.; Zeng, J.; Zhuang, Z.; Gan, S.; Cai, Y.; Guo, J.; Su, S.-J.; Zhao, Z.; Tang, B. Z. Highly Efficient Nondoped OLEDs with Negligible Efficiency Roll-Off Fabricated from Aggregation-Induced Delayed Fluorescence Luminogens. *Angew. Chem., Int. Ed.* **2017**, *56*, 12971−12976.
(45) Liu, H.; Zeng, J.; Guo, J.; Nie, H.; Zhao, Z.; Tang, B. Z. High-Performance Non-Doped OLEDs with Nearly 100% Exciton Use and Negligible Efficiency Roll-Off. *Angew. Chem., Int. Ed.* **2018**, *57*, 9290−9294.
(46) Gan, S.; Luo, W.; He, B.; Chen, L.; Nie, H.; Hu, R.; Qin, A.; Zhao, Z.; Tang, B. Z. Integration of Aggregation-Induced Emission and Delayed Fluorescence into Electronic Donor-Acceptor Conjugates. *J. Mater. Chem. C* **2016**, *4*, 3705−3708.
(47) Zhang, Q.; Li, J.; Shizu, K.; Huang, S.; Hirata, S.; Miyazaki, H.; Adachi, C. Design of Efficient Thermally Activated Delayed Fluorescence Materials for Pure Blue Organic Light Emitting Diodes. *J. Am. Chem. Soc.* **2012**, *134*, 14706−14709.
(48) Liu, B.; Nie, H.; Lin, G.; Hu, S.; Gao, D.; Zou, J.; Xu, M.; Wang, L.; Zhao, Z.; Ning, H.; Peng, J.; Cao, Y.; Tang, B. Z. High-Performance Doping-Free Hybrid White OLEDs Based on Blue Aggregation-Induced Emission Luminogens. *ACS Appl. Mater. Interfaces* **2017**, *9*, 34162−34171.
(49) Zhen, S.; Wang, S.; Li, S.; Luo, W.; Gao, M.; Ng, L. G.; Goh, C. C.; Qin, A.; Zhao, Z.; Liu, B.; Tang, B. Z. Efficient Red/Near-Infrared Fluorophores Based on Benzo[1,2-b:4,5-b′]dithiophene 1,1,5,5-Tetraoxide for Targeted Photodynamic Therapy and in vivo Two-Photon Fluorescence Bioimaging. *Adv. Funct. Mater.* **2018**, *28*, 1706945.
(50) Chen, B.; Liu, B.; Zeng, J.; Nie, H.; Xiong, Y.; Zou, J.; Ning, H.; Wang, Z.; Zhao, Z.; Tang, B. Z. Efficient Bipolar Blue AIEgens for High-Performance Nondoped Blue OLEDs and Hybrid White OLEDs. *Adv. Funct. Mater.* **2018**, *28*, 1803369.
(51) Holmes, R. J.; Forrest, S. R.; Tung, Y.-J.; Kwong, R. C.; Brown, J. J.; Garon, S.; Thompson, M. E. Blue organic electrophosphorescence using exothermic host-guest energy transfer. *Appl. Phys. Lett.* **2003**, *82*, 2422−2424.
(52) Jeong, H.; Shin, H.; Lee, J.; Kim, B.; Park, Y.-I.; Yook, K. S.; An, B.-K.; Park, J. Recent Progress in the Use of Fluorescent and Phosphorescent Organic Compounds for Organic Light-Emitting Diode Lighting. *J. Photonics Energy* **2015**, *5*, 057608.
(53) Wang, S.; Lee, C. W.; Lee, J. Y.; Hwang, S.-H. Synthesis and green phosphorescent OLED device performance of cyanofluorene-linked phenylcarbazoles as host material. *New J. Chem.* **2018**, *42*, 5059−5065.
(54) Li, S.-H.; Wu, S.-F.; Wang, Y.-K.; Liang, J.-J.; Sun, Q.; Huang, C.-C.; Wu, J.-C.; Liao, L.-S.; Fung, M.-K. Management of Excitons for Highly Efficient Organic Light-Emitting Diodes with Reduced Triplet Exciton Quenching: Synergistic Effects of Exciplex and Quantum Well Structure. *J. Mater. Chem. C* **2018**, *6*, 342−349.
(55) Yook, K. S.; Lee, J. Y. Small Molecule Host Materials for Solution Processed Phosphorescent Organic Light-Emitting Diodes. *Adv. Mater.* **2014**, *26*, 4218−4233.
(56) Sasabe, H.; Kido, J. Recent Progress in Phosphorescent Organic Light-Emitting Devices. *Eur. J. Org. Chem.* **2013**, 7653−7663.

DOI: 10.1021/acsami.9b06995
ACS Appl. Mater. Interfaces 2019, 11, 27134−27144

(57) Lei, G.; Wang, L.; Qiu, Y. Multilayer Organic Electrophosphorescent White Light-Emitting Diodes without Exciton-Blocking Layer. *Appl. Phys. Lett.* **2006**, *88*, 103508.
(58) Tsuboi, T.; Murayama, H.; Yeh, S.-J.; Wu, M.-F.; Chen, C.-T. Photoluminescence Characteristics of Blue Phosphorescent Ir3^{+}-Compounds FIrpic and FIrN_4 Doped in *m*CP and SimCP. *Opt. Mater.* **2008**, *31*, 366−371.
(59) Lai, S. L.; Tao, S. L.; Chan, M. Y.; Ng, T. W.; Lo, M. F.; Lee, C. S.; Zhang, X. H.; Lee, S. T. Efficient White Organic Light-Emitting Devices Based on Phosphorescent Iridium Complexes. *Org. Electron.* **2010**, *11*, 1511−1515.
(60) Kim, M.; Lee, J. Y. Engineering the Substitution Position of Diphenylphosphine Oxide at Carbazole for Thermal Stability and High External Quantum Efficiency above 30% in Blue Phosphorescent Organic Light-Emitting Diodes. *Adv. Funct. Mater.* **2014**, *24*, 4164−4169.
(61) Liu, H.; Cheng, G.; Hu, D.; Shen, F.; Lv, Y.; Sun, G.; Yang, B.; Lu, P.; Ma, Y. A Highly Efficient, Blue-Phosphorescent Device Based on a Wide-Bandgap Host/FIrpic: Rational Design of the Carbazole and Phosphine Oxide Moieties on Tetraphenylsilane. *Adv. Funct. Mater.* **2012**, *22*, 2830−2836.
(62) Wang, F.; Liu, D.; Li, J.; Ma, M. Modulation of n-Type Units in Bipolar Host Materials toward High-Performance Phosphorescent OLEDs. *ACS Appl. Mater. Interfaces* **2017**, *9*, 37888−37897.
(63) Lin, M.-S.; Yang, S.-J.; Chang, H.-W.; Huang, Y.-H.; Tsai, Y.-T.; Wu, C.-C.; Chou, S.-H.; Mondal, E.; Wong, K.-T. Incorporation of a CN Group into *m*CP: A New Bipolar Host Material for Highly Efficient Blue and White Electrophosphorescent Devices. *J. Mater. Chem.* **2012**, *22*, 16114−16120.
(64) Fukagawa, H.; Yokoyama, N.; Irisa, S.; Tokito, S. Pyridoindole Derivative as Electron Transporting Host Material for Efficient Deep-blue Phosphorescent Organic Light-emitting Diodes. *Adv. Mater.* **2010**, *22*, 4775−4778.
(65) Takizawa, S.-y.; Montes, V. A.; Anzenbacher, P., Jr. Phenylbenzimidazole-Based New Bipolar Host Materials for Efficient Phosphorescent Organic Light-Emitting Diodes. *Chem. Mater.* **2009**, *21*, 2452−2458.
(66) Jiang, W.; Duan, L.; Qiao, J.; Dong, G.; Wang, L.; Qiu, Y. Tuning of Charge Balance in Bipolar Host Materials for Highly Efficient Solution-Processed Phosphorescent Devices. *Org. Lett.* **2011**, *13*, 3146−3149.
(67) Swensen, J. S.; Polikarpov, E.; Von Ruden, A.; Wang, L.; Sapochak, L. S.; Padmaperuma, A. B. Improved Efficiency in Blue Phosphorescent Organic Light-Emitting Devices Using Host Materials of Lower Triplet Energy than the Phosphorescent Blue Emitter. *Adv. Funct. Mater.* **2011**, *21*, 3250−3258.
(68) Murgatroyd, P. N. Dimensional Considerations for Space-Charge Conduction in Solids. *J. Phys. D: Appl. Phys.* **1970**, *3*, 1488−1490.
(69) Ogawa, T.; Cho, D.-C.; Kaneko, K.; Mori, T.; Mizutani, T. Numerical Analysis of the Carrier Behavior of Organic Light-Emitting Diode: Comparing a Hopping Conduction Model with a SCLC Model. *Thin Solid Films* **2003**, *438*−*439*, 171−176.
(70) Jeon, W. S.; Park, T. J.; Kim, S. Y.; Pode, R.; Jang, J.; Kwon, J. H. Ideal Host and Guest System in Phosphorescent OLEDs. *Org. Electron.* **2009**, *10*, 240−246.
(71) Sun, N.; Wang, Q.; Zhao, Y.; Chen, Y.; Yang, D.; Zhao, F.; Chen, J.; Ma, D. High-Performance Hybrid White Organic Light-Emitting Devices without Interlayer between Fluorescent and Phosphorescent Emissive Regions. *Adv. Mater.* **2014**, *26*, 1617−1621.

DOI: 10.1021/acsami.9b06995
ACS Appl. Mater. Interfaces 2019, 11, 27134−27144